Atmos. Chem. Phys., 19, 8175–8187, 2019
https://doi.org/10.5194/acp-19-8175-2019

Atmospheric Chemistry and Physics
Open Access
EGU

Influence of functional groups on toxicity of carbon nanomaterials

Yongchun Liu[1,2], Haotian Jiang[2,4], Chunmei Liu[3], Yanli Ge[2], Lian Wang[2], Bo Zhang[2], Hong He[2,4,5], and Sijin Liu[2,4]

[1]Aerosol and Haze Laboratory, Advanced Innovation Center for Soft Matter Science and Engineering, Beijing University of Chemical Technology, Beijing, 100029, China
[2]State Key Joint Laboratory of Environment Simulation and Pollution Control, Research Center for Eco-Environmental Sciences, Chinese Academy of Sciences, Beijing, 100085, China
[3]Bioduro Technology (Beijing) Co., Ltd., Beijing, 102200, China
[4]University of the Chinese Academy of Sciences, Beijing, 100049, China
[5]Center for Excellence in Urban Atmospheric Environment, Institute of Urban Environment, Chinese Academy of Sciences, Xiamen 361021, China

Correspondence: Y. Liu (liuyc@buct.edu.cn) and S. Liu (sjliu@rcees.ac.cn)

Received: 31 December 2018 – Discussion started: 15 February 2019
Revised: 25 April 2019 – Accepted: 5 June 2019 – Published: 24 June 2019

Abstract. It has been recognized that carbon nanomaterials and soot particles are toxic for human health, but the influence of functionalization on their toxicity as well as the evolution of the toxicity of carbon nanomaterials due to chemical aging in the atmosphere is still controversial. In the current study, the oxidation potential measured by dithiothreitol (DTT) decay rate and the cytotoxicity to murine macrophage cells of different functionalized carbon nanomaterials were investigated to understand the role of functionalization in their toxicities. The DTT decay rates of special black 4A (SB4A), graphene, graphene oxide, single-walled carbon nanotubes (SWCNTs), SWCNT-OH and SWCNT-COOH were 45.9 ± 3.0, 58.5 ± 6.6, 160.7 ± 21.7, 38.9 ± 8.9, 57.0 ± 7.2 and 36.7 ± 0.2 pmol min^{-1} μg^{-1}, respectively. Epoxide was found to be mainly responsible for the highest DTT decay rate of graphene oxide compared to other carbon nanomaterials based on comprehensive characterizations. Both carboxylation and hydroxylation showed little influence on the oxidation potential of carbon nanomaterials, while epoxidation contributes to the enhancement of oxidation potential. All these carbon nanomaterials were toxic to the murine J774 cell line. However, oxidized carbon nanomaterials (graphene oxide, SWCNT-OH and SWCNT-COOH) showed weaker cytotoxicity to the J774 cell line compared to the corresponding control sample as far as the metabolic activity was considered and stronger cytotoxicity to the J774 cell line regarding the membrane integrity and DNA incorporation. These results imply that epoxidation might enhance the oxidation potential of carbon nanomaterials.

1 Introduction

Carbon nanomaterials are predominantly composed of carbon atoms, only one kind of element, but they have largely diverse structures characterized by different degrees of crystallinity and different macro- and micromorphology (Somiya, 2013). Their basic structure is that of graphite with planes of honeycomb-structured carbon atoms. Carbon black (CB), which is produced from incomplete combustion of heavy petroleum materials under controlled conditions (Apicella et al., 2003), has been widely used in industrial products, such as inkjet printer ink, rubber and plastic products (Lee et al., 2016); electrically conductive plastics (Parant et al., 2017); paints, coatings and cosmetics (Sanders and Peeten, 2011); and so on. CB is a quasi-graphitic form of nearly pure elemental carbon (EC, consists of graphene layers). It is distinguished by its very low quantities of extractable organic compounds and total inorganics (Long et al., 2013) compared to soot or black carbon (BC) (Andreae and Gelencser, 2006). Soot, which originates from incomplete combustion of biomass, biofuels, fossil fuels and natural fires in reduced or anoxic environments, is a mixture of elemental carbon and organic carbon (OC) compounds (Muckenhuber and Grothe, 2006). In addition, as a class of engineering nanoparticles, carbon nanotubes (CNTs) and graphene materials are also a large group of carbon nanomaterials although their graphene sheets are arranged more regularly (Hu et al., 2010) than in CB (Nienow and Roberts, 2006). During production and use of these as consumer prod-

ucts, they are prone to enter the environment and ultimately the human body (Helland et al., 2007; Tiwari and Marr, 2010), and subsequently to pose a risk of adverse health effects.

The adverse effect of CB and soot particles on human health has attracted much attention in the atmospheric chemistry community (Baumgartner et al., 2014). Overall, exposure to CB is associated with a high risk of cancer, respiratory and cardiovascular diseases (WHO, 2013; Niranjan and Thakur, 2017). Mitochondrial damage in alveolar macrophages and bronchial epithelial cells resulting from exposure to diesel exhaust particles (DEPs) has been observed (Li et al., 2002a, b). Oxidation stress or reactive oxygen species (ROS) generation is one of the mechanisms related to the toxicity of particles including soot particles (Nel et al., 2006), and has been even used as a paradigm to assess particle toxicity (Xia et al., 2006).

Dithiothreitol (DTT) decay rate is commonly used as a cell-free measure of the oxidative potential of different particles (Cho et al., 2005; Charrier and Anastasio, 2012; Kumagai et al., 2002), such as ambient particles (Li et al., 2003; Fang et al., 2016; Cho et al., 2005; Charrier and Anastasio, 2012; Wang et al., 2013), secondary organic aerosol (SOA) (McWhinney et al., 2013b), DEP (Li et al., 2009; McWhinney et al., 2013a), carbon nanotubes (CNTs) (Liu et al., 2015), flame soot (Antinolo et al., 2015; Holder et al., 2012; Li et al., 2013) and commercial carbon black (CB) particles (Koike and Kobayashi, 2006; Li et al., 2009, 2015, 2013). However, the reported DTT decay rate of soot and CB particles varied substantially from 0.9 to $\sim 50\,\mathrm{pmol\,min^{-1}\,\mu g^{-1}}$. The variation in DTT decay rate among different samples implies the importance of the composition or structure of particles in their toxicities.

Although transition metals, elemental carbon, humic-like substances and quinones are responsible for ROS generation on particle surfaces (McWhinney et al., 2013b; Li et al., 2003), more work is still required to deeply understand the toxicity of soot and the reason why the toxicity varies greatly among different soot samples. On the other hand, soot particles are prone to undergo oxidation by O_3, OH, NO_x etc. during transport in the atmosphere. Subsequently, functionalization including formation of OH, C=O, epoxide (C−O−C) and COOH occurs (Mawhinney et al., 2000; Liu et al., 2015; Holder et al., 2012; Corbin et al., 2015). This makes it more complicated to understand the toxicity of soot particles. For example, several studies have found that atmosphere-relevant oxidation of CB or soot by O_3 leads to enhancement of their oxidative potential (Li et al., 2009, 2013, 2015; Antinolo et al., 2015; Holder et al., 2012). In particular, the DTT decay rate of soot particles were found to increase as a function of the content of quinone formed via ozone oxidation of organic carbons in soot (Antinolo et al., 2015). However, some other studies found that oxidation of CB or soot by O_3 or OH under atmosphere-related conditions has little influence on their oxidative potential or cytotoxicity although surface functionalization is observable (Liu et al., 2015; Peebles et al., 2011). Therefore, it is necessary to understand the role of functional groups in the toxicity of soot and CB particles.

During the combustion process, however, multiple functional groups including OH, C=O, COOH, esters, ethers, etc. are usually formed at the same time and present in both OC and EC (Han et al., 2012a; Cain et al., 2010; Wal et al., 2011; Popovicheva et al., 2015). Thus, it is difficult to differentiate the role of one kind of functional group from others in the toxicity of soot particles. However, it is possible to investigate the role of functional groups in the toxicity of carbon nanomaterials when using CB or engineered carbon particles with different functional groups as model samples of soot particles. Actually, it has been recognized that the surface properties of carbon nanomaterials will influence their biological effects or toxicity (Lara-Martinez et al., 2017; Y. Liu et al., 2014; Koromilas et al., 2014). For example, a recent study has found that hydrated graphene oxide exhibited a higher cytotoxicity to THP-1 (a human monocytic leukemia cell line) and BEAS-2B (human bronchial epithelial) cells as a consequence of lipid peroxidation of the surface membrane and membrane lysis compared to pristine and reduced graphene oxide (Li et al., 2018). Functionalized multiwalled carbon nanotubes (FMWCNTs) are highly cardioembryotoxic in comparison to functionalized oxygen-doped multiwalled carbon nanotubes (Lara-Martinez et al., 2017). As pointed out by Lara-Martinez et al. (2017), however, cytotoxic effects of carbon nanomaterials at the cellular level generate considerable controversy and more research is clearly needed to gain insight into the mechanism of these adverse effects. In addition, passive diffusion and energy-dependent endocytosis are the two methods suggested for particles entry into living cells (Foroozandeh and Aziz, 2018). They can also be distributed to various parts of the body from where they can either remain, translocate or be excreted. Therefore, it is meaningful to separately investigate the influence of functionalization on other endpoints even for these carbon nanomaterials.

In the current study, both the cell-free toxicity and the cell cytotoxicity of carbon nanomaterials with different functionalities were evaluated to focus on the role of functionalization in their toxicities. DTT decay rates representing the oxidative potential and the cytotoxicity of murine macrophage cells were investigated. The carbon nanomaterials were characterized with inductively coupled plasma mass spectrometry (ICP-MS), thermal gravimetric analysis (TGA), X-ray photoelectron spectroscopy (XPS), transmission electron microscopy (TEM) and a zeta-potential analyzer. The role of oxygen-containing species in the toxicity of carbon nanomaterials was discussed. This work will be helpful for understanding the toxicity of carbon nanomaterials with different functional groups.

2 Experimental section

2.1 Chemicals and characterization of particle samples

Commercial carbon nanomaterials including Special Black 4A (SB4A), graphene, graphene oxide, SWCNT, SWCNT-OH and SWCNT-COOH were used in this study. All these functional groups have been identified in soot particles and chemically aged soot or CB particles. SB4A was supplied by Degussa. The other carbon nanomaterials with purity $> 98\,\%$ were supplied by Timesnano. To obtain graphene oxide with low epoxide content, graphene oxide was thermally treated at 200 °C for 30 min in a high-purity (99.999 %) nitrogen flow. Dithiothreitol (DTT) was supplied by Sigma-Aldrich. 5,5'-dithiobis-(2-nitrobenzoic acid) (DTNB) was obtained from Alfa Aesar. Standard solutions of metal ions including Cr, Mn, Fe, Co, Ni, Cu, Zn, Cd, As, Sn and Pb were supplied by the National Institute of Metrology, China. A 30 % H_2O_2 solution was supplied by Sinopharm Chemical Reagent Co., Ltd.

A transmission electron microscope (H-7500, Hitachi) was used to investigate the morphologies of carbon nanomaterials (Golberg et al., 2012). Particles were ultrasonically dispersed in ultrapure water (18 MΩ) and a droplet of suspending liquid was deposited onto a Cu microgrid. An acceleration voltage of 80 kV was used for measurements. The morphologies are shown in Fig. S1 in the Supplement. The diameters of primary particles were analyzed by ImageJ 1.41 software (Liu et al., 2010). The diameter of the primary carbon sphere for SB4A was 66 ± 17 nm. The outer diameter (OD) of SWCNT, SWCNT-OH and SWCNT-COOH were < 2 nm with fiber lengths of 1–3 µm according to the product report and also confirmed by TEM (Fig. S1). Graphene and graphene oxide are two-dimensional materials with monolayers and diameters of 0.5–3 µm.

XPS were measured using an AXIS Supra/Ultra (Kratos, Kratos Analytical Ltd.) to identify the oxygen-containing species on the surface of carbon nanomaterials (Wal et al., 2011; Schuster et al., 2011). The samples were excited by Al Kα X-rays ($h\upsilon = 1486.7$ eV) with 15 kV of working voltage and 40 mA of emission current. The spectra were analyzed with XPSPeak software. The content of organic carbon (OC) in carbon nanomaterials was measured by thermal desorption using a commercial thermogravimetric instrument (TGA/DSC1/HT1600, Mettler Toledo Co., Ltd.). The amount of OC lost from the particles was recorded when the temperature was ramped from 30 to 300 °C at 10 °C min^{-1} in nitrogen flow according to the protocol reported in previous work (Han et al., 2012a). Metals in the particles were measured with an inductively coupled plasma mass spectrometer (ICP-MS 7500a, Agilent Technologies) after being digested with a concentrated 1 : 3 HNO_3/HCl. Transition metals were quantified with the standard solution. Zeta potentials of the carbon nanomaterials were measured after sonicating for 30 min in ultrapure water (18.2 MΩ) by using a nanoparticle size and zeta-potential analyzer (Zetasizer Nano, ZS90).

2.2 DTT assay test

The DTT assay is an indirect chemical assay used for measuring the redox cycling capacity of PM (particulate matter; Xia et al., 2006). The added DTT is oxidized to its disulfide form by ROS in particulate matter (Kumagai et al., 2002). Thus, the rate of DTT consumption is proportional to the concentration of ROS in the sample (Cho et al., 2005). In this study, ~ 150 µg of carbon nanomaterials was suspended in 10.0 mL phosphate buffer (0.1 M, pH 7.4) and sonicated for 15 min. Then 2.0 mL of 0.5 mM DTT solution was added to 3.0 mL aliquots of the sonicated suspensions. A redox reaction took place in a thermostat shaking chamber at 37 °C. The remaining DTT concentration was measured every 15 min by adding 0.25 mL of the reaction mixture filtration to 1.0 mL of 0.25 mM DTNB solution. DTNB reacted with the thiol groups in DTT to form a yellow compound (2-nitro-5-thiobenzoate, NTB), which could be detected by a UV–vis absorption spectrometer (723N, Shanghai Ruiting Network Technology Co., Ltd.) at 412 nm. Then, the amount of DTT consumed by PM was calculated according to the standard curves of DTT. The loss rate of DTT via a redox reaction in the presence of PM was monitored as the decrease in DTT concentration and normalized to the particle mass. Blank experiments were carried out without carbon nanomaterial particles in the buffer solution. For some samples, the response to the DTT assay was also measured for the water-soluble components of SWCNT by filtering aliquots of the samples with a 0.22 µm PTFE syringe filter and measuring the activity of the solution without particles.

2.3 In vitro assays

Carbon nanomaterial particles were dispersed with 0.025 % Tween-80 in 0.19 % NaCl solution using a Dounce glass homogenizer, followed by sonication. A homogeneous and stable suspension of SWCNTs was obtained after the sonication process. Cytotoxicity assessment of carbon nanomaterials was carried out using murine J774 cells. Three different assays targeting distinct mechanisms of cellular metabolic perturbations were assessed simultaneously, including ATP (adenosine triphosphate, energy metabolism), LDH (lactate dehydrogenase, membrane integrity) and BrdU (bromodeoxyuridine, incorporation into DNA) assays. The experiments were carried out according to the corresponding protocol. Briefly, 4×10^5 cells mL^{-1} (J774 cells) was exposed to carbon particles in 96-well plates for 24 h for ATP and LDH assays, while the initial J774 cell concentration was 2×10^5 cells mL^{-1} for the BrdU assay. Carbon nanomaterials were dosed at 0, 10, 30 and 100 µg cm^{-2} in a final volume of 200 µL per well as similar to that reported in literature (Kumarathasan et al., 2014, 2012). The luminescence

spectroscopy of the supernatant after centrifugal separation at 1000 rpm for 5 min was measured after 24 h of cell exposure using a multimode microplate reader (Varioskan® Flash, Thermo Fisher Scientific). The zero dose of carbon nanomaterials refers to the blank experiment and also means a toxicity of 0.025 % Tween-80 alone in 0.19 % NaCl solution. Similar to the literature results (Hadrup et al., 2017), it did not incur any obvious deleterious effect on cell growth. In addition, it has been well recognized that carbon nanoparticles tended to aggregate in water even after ultrasonic dispersion. Tween-80 was verified to be a biocompatable dispersant for carbon black (Kim et al., 2012). Negative control experiments were performed in wells containing medium without cells to obtain a value for background luminescence. Positive control experiments were carried out with H_2O_2 solution for LDH assays (Fig. S2).

3 Results

3.1 Oxidative potential of carbon nanomaterials

Figure 1 shows the DTT decay rates of SB4A, graphene, graphene oxide, SWCNT, SWCNT-OH and SWCNT-COOH. They were 45.9 ± 3.0, 58.5 ± 6.6, $160.7.0 \pm 21.7$, 38.9 ± 8.9, 57.0 ± 7.2 and 36.7 ± 0.2 pmol min^{-1} μg^{-1}, respectively. Except for graphene oxide, the measured DTT decay rates for these carbon nanomaterials (with mean value of 47.4 ± 10.1 pmol min^{-1} μg^{-1}) were comparable with the DTT loss rates of soot reported in the literature. For example, it was 36.2 ± 4.9 pmol min^{-1} μg^{-1} for Printex U (Li et al., 2015) and 59.3 ± 7.4 pmol min^{-1} for typical soot particles, such as 33.6 pmol min^{-1} μg^{-1} for methane flame soot (Holder et al., 2012), 49 ± 7 pmol min^{-1} μg^{-1} for propane flame soot (Antinolo et al., 2015), 27.0 pmol min^{-1} μg^{-1} for hexane flame soot (Li et al., 2013), as well as the typical ambient $PM_{2.5}$ particles (34.7 ± 19.1 pmol min^{-1} μg^{-1}) (Charrier and Anastasio, 2012; Q. Liu et al., 2014). However, the measured DTT decay rates for these carbon nanomaterials were significantly higher than those of diesel soot (6.1 pmol min^{-1} μg^{-1}) and graphite (0.9 pmol min^{-1} μg^{-1}) (Li et al., 2013) reported in previous work. It should be noted that the DTT decay rate of graphene oxide measured in this study was 160.7 ± 21.7 pmol min^{-1} μg^{-1}. Based on a T test, the DTT decay rate of graphene oxide was significantly higher than that of other tested carbon nanomaterials at the 0.05 level ($t = 8.498$, which is greater than the critical value of 2.447). This means that graphene oxide definitely has a stronger oxidative potential than other CB or carbon nanomaterials in this work.

3.2 Cytotoxicity of carbon nanomaterials to the murine J774 cell line

At the present time, the A549 (a human adenocarcinomic alveolar epithelial cell) and THP-1 cell lines are usually chosen as target cell lines (Kumarathasan et al., 2012, 2014; Liu et al., 2015) to evaluate the alveolar and pulmonary toxicity of CB particles. As the first barrier of the immune system, macrophage cell lines will fight against the invaded particles in the lungs. Macrophage cell lines like J774 cells are ideal model systems for establishing the biophysical foundations of autonomous deformation and motility of immune cells (Lam et al., 2009). It has been found that CB nanoparticles are able to stimulate the release of macrophage chemoattractants when exposed to type II epithelial cell lines (L-2 cells) at subtoxic doses (Barlow et al., 2005). CNT exposure can also lead to biological changes in J774 cells (Kumarathasan et al., 2012). Therefore, it is meaningful to investigate the cytotoxicity of different carbon nanomaterials as well as the influence of surface functional groups on the macrophage cell lines.

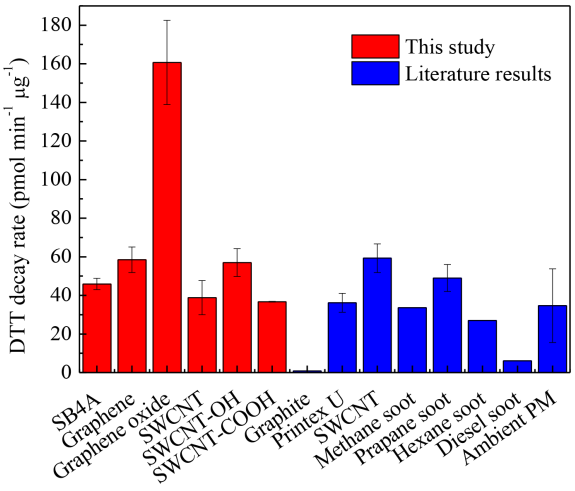

Figure 1. DTT decay rates of several black carbon materials compared with literature results (Li et al., 2013, 2015; Charrier and Anastasio, 2012; Q. Liu et al., 2014a; Liu et al., 2015; Holder et al., 2012; Antinolo et al., 2015).

Figure 2 shows the in vitro toxicities of SB4A, graphene, graphene oxide, SWCNT, SWCNT-COOH and SWCNT-OH. The stars mean that the indicator of toxicity at a certain dose of carbon nanomaterials is significantly different from the corresponding blank experiments at the 0.05 level. As shown in Fig. 2, the metabolic activity of the J774 cell line decreased monotonously as a function of the dose of all these carbon nanomaterials. The relative ATP level (1.01 ± 0.02) at the SB4A dose of 10 μg cm^{-2} was almost the same as that of the blank sample, while it significantly decreased to 0.89 ± 0.05 and 0.61 ± 0.07 when the dose of SB4A increased to 30 and 100 μg cm^{-2}, respectively. Similarly, the relative ratio of BrdU incorporation decreased from 0.74 ± 0.03 to 0.60 ± 0.04 when the dose of SB4A increased from 30 to 100 μg cm^{-2}. However, the released LDH levels were constant within experimental uncertainty at different SB4A doses.

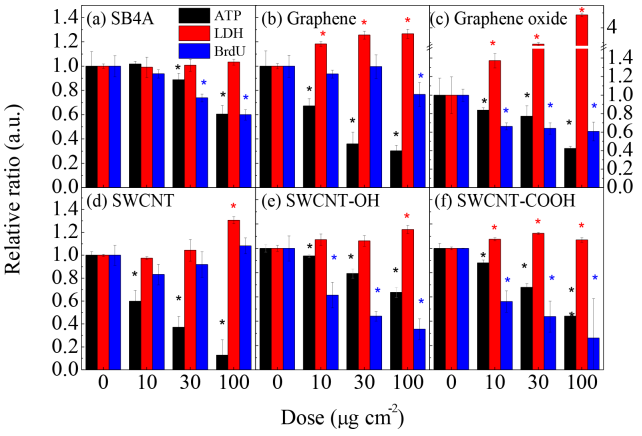

Figure 2. Cytotoxicity of **(a)** SB4A, **(b)** graphene, **(c)** graphene oxide, **(d)** SWCNT, **(e)** SWCNT-OH and **(f)** SWCNT-COOH toward the murine J774 cell line. The stars mean the difference is significant at 0.05 level for a certain dose of carbon nanomaterials compared to the corresponding blank experiments.

As shown in Fig. 2b–f, the metabolic activity of murine J774 cells decreased more significantly when exposed to engineered carbon nanomaterials than SB4A. For example, the relative ratio of ATP level was 0.67 ± 0.06, 0.84 ± 0.03, 0.59 ± 0.10, 0.93 ± 0.01 and 0.88 ± 0.02 even when the J774 cells were exposed to $10\,\mu g\,cm^{-2}$ of graphene, graphene oxide, SWCNT, SWCNT-OH and SWCNT-COOH, respectively. When exposed to high doses of engineered carbon nanomaterials, the reduction of relative ATP level became more significant. These results mean the cytotoxicity of the engineered carbon nanomaterials studied in this work are stronger than that of SB4A regarding metabolic activity. Graphene, graphene oxide and SWCNT-COOH significantly enhanced the release of LDH at different exposure levels, while SWCNT and SWCNT-OH only led to significant increases of released LDH at high exposure level ($100\,\mu g\,cm^{-2}$).

It should be noted that the reduction of ATP ratio of J774 cells exposed to graphene oxide was weaker than that of graphene. The reduction of ATP ratio of J774 cells exposed to SWCNT-OH or SWCNT-COOH was also weaker than that of SWCNT. However, compared with graphene, graphene oxide showed a much stronger toxicity to J774 cells as far as the membrane integrity was considered. The released LDH at an exposure level of $30\,\mu g\,cm^{-2}$ of graphene oxide was comparable with that when exposed to 150 ppm H_2O_2 (Fig. S2). In addition, graphene oxide, SWCNT-OH and SWCNT-COOH significantly inhibited DNA synthesis of J774 cells when the carbon nanomaterial doses were above $10\,\mu g\,cm^{-2}$, while graphene and SWCNT did not show significant inhibition of DNA synthesis for J774 cells. For instance, the relative ratio of BrdU when J774 cells were exposed to $100\,\mu g\,cm^{-2}$ of graphene oxide was 0.61 ± 0.10, while it was 0.77 ± 0.10 for graphene-exposed cells at the same exposure level. They were 0.62 ± 0.10 for SWCNT-OH-treated cells and 0.56 ± 0.09 for SWCNT-COOH-treated cells at a dose of $10\,\mu g\,cm^{-2}$ compared to 0.83 ± 0.09 for $10\,\mu g\,cm^{-2}$ of SWCNT-treated J774 cells.

3.3 Characterization of carbon nanomaterials

As shown in Fig. S1, the morphologies of these carbon nanomaterials varied greatly. SB4A is a zero-dimensional material. SWCNT, SWCNT-OH and SWCNT-COOH are one-dimensional materials. Graphene and graphene oxide were two-dimensional materials.

The content of transition metals including Cr, Fe, Mn, Co, Ni, Cu, Zn, As, Cd, Sn and Pb were measured by using an ICP-MS after the carbon nanomaterials were digested with 1 : 3 HNO_3/HCl. As shown in Fig. S4A, Fe was the most abundant transition metal in these carbon nanomaterials. Its concentration varied from 122 to $6596\,\mu g\,g^{-1}$ among different carbon nanomaterials. The concentration of other metals varied from zero to several hundred micrograms per gram ($\mu g\,g^{-1}$) depending on both carbon nanomaterials and the type of metals. Compared with SB4A, these engineered carbon nanomaterials showed higher metal contents. For example, the total metal content in graphene was 6 times as high as that in SB4A, while it was 33 times as high in SWCNT as that in SB4A. This can be explained by the fact that graphene and SWCNT materials were catalytically synthesized using metal catalysts containing Fe, Co or Ni (Maruyama, 2018).

Figure 3 shows the thermogravimetric and differential thermal analysis curves for these CB materials when the temperature was ramped from 30 to 300 °C at $10\,°C\,min^{-1}$ in nitrogen flow. Weight loss (Fig. 3a) accompanied with an endothermic process (Fig. 3b) was observed below 60 °C for all of these samples. This can be ascribed to desorption of surface adsorbents including bonded organics and trace water. As shown in Fig. 3b, the saddle points of these differential thermal analysis curves were observed at 35, 35, 41, 42, 56 and 58 °C for graphene, SWCNT, SB4A, SWCNT-OH, SWCNT-COOH and graphene oxide, respectively. It should be noted that the oxidized carbon nanomaterials such as SWCNT-OH, SWCNT-COOH and graphene oxide showed higher saddle points of the heat curves than graphene, SWCNT and SB4A. This implies stronger a interaction between the adsorbents and these three oxidized carbon nanomaterials compared with the counterpart. Therefore, it is reasonable to deduce that the adsorbed water mainly contributes to the weight loss at this stage. The sample weight slightly decreased as the temperature further increased for all of these carbon nanomaterials except for graphene oxide and accompanied with a gradual increase in the heat flow. This can be ascribed to desorption of adsorbed organics from the surface of the carbon nanomaterials. The relatively low increase rate of heat at this stage was consistent with the small heat capacity of organics when compared with the first one, which was ascribed to desorption

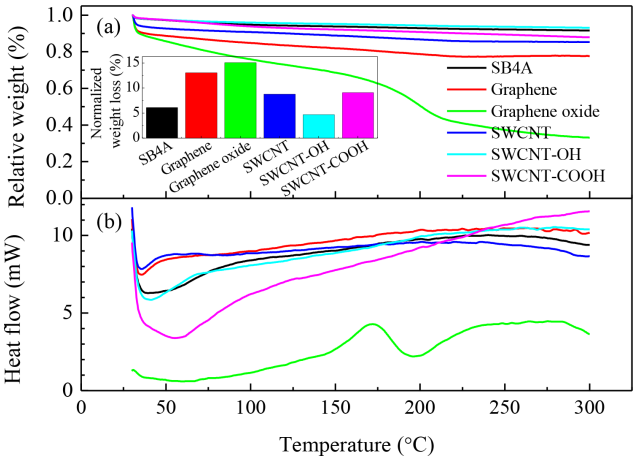

Figure 3. (a) Thermogravimetric curves of carbon nanomaterials in nitrogen gas flow; **(b)** the corresponding differential thermal analysis curves. The inset graph shows the weight loss due to desorption of organics.

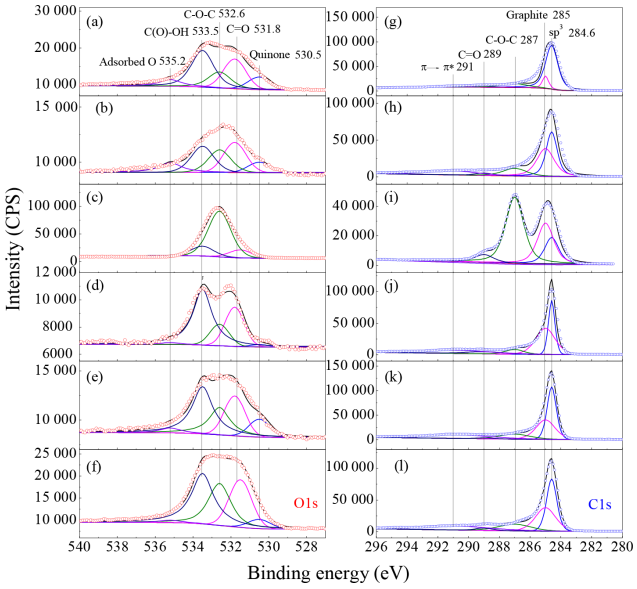

Figure 4. XPS spectra of carbon nanomaterials. **(a)–(f)** are O1s spectra and **(g)–(l)** are C1s spectra for SB4A, graphene, graphene oxide, SWCNT, SWCNT-OH and SWCNT-COOH, respectively.

of water. For graphene oxide, however, significant weight loss (from 32 % to 60 %) was observed and was accompanied with an acute exothermic process when the temperature increased from 150 to 200 °C as shown in Fig. 3b. This implies that a release of pyrolysis products and structural collapse of graphene oxide occurred. It also means a high reactivity of graphene oxide and highlights the distinctive property of graphene oxide among these investigated carbon nanomaterials. The adsorbed organics were estimated based on the thermogravimetric curves when the possible contribution of water was ruled out. For graphene oxide, 150 °C was taken as the endpoint, while 300 °C was chosen for other samples. The contents of adsorbed organics on SB4A, graphene, graphene oxide, SWCNT, SWCNT-OH and SWCNT-COOH were 6 %, 13 %, 15 %, 9 %, 5 % and 9 %, respectively.

To further investigate the role of surface oxygen in the toxicity of carbon nanomaterials, the oxygen-containing species of these carbon nanomaterials were identified with X-ray photoelectron spectroscopy. Figure 4 shows the typical O1s and C1s spectra of these carbon nanomaterials. Several oxygen-containing species were observed as shown in Fig. 4a–f. Adsorbed oxygen was observed at 535.2 eV in the O1s spectra. The carbon–oxygen single bond in hydroxyl group (C−OH) and epoxide (C−O−C) were at 533.5 and 532.6 eV, respectively. The carbon–oxygen double bound (C=O) was observed at 531.8 eV, while the highly conjugated form of carbonyl oxygen such as quinone groups was identified at 530.5 eV (Schuster et al., 2011). In the C1s spectra (Fig. 4g–l), the band at 291 eV was attributed to the shakeup peak associated with a π–π^* transition (Simmons et al., 2006). The band at 289 eV corresponded to carbonyls and epoxides was observed at 287 eV (Kuznetsova et al., 2001). The bands at 285 and 284.6 eV were assigned to graphite and sp^3 carbon, respectively. In particular, the intensity of the C−O−C band at 532.6 eV in graphene oxide was very strong compared to other carbon nanomaterials. At the same time, the band of C−O−C at 287 eV was also much stronger than that of other carbon nanomaterials in the C1s spectrum. These results mean that epoxide (C−O−C) is the predominating species (Fig. 5c and i) in graphene oxide. It should be noted that XPS results only represent the surface atom ratios, which are different from the OC content representing the bulk composition. However, the surface property of a particle is very important to understand the toxicity of nanoparticles from the point of view of particle–cell interaction (Cedervall et al., 2007).

4 Discussion

As shown in Fig. 2, all carbon nanomaterials showed decreased ATP activities as a function of the dose. This means that the carbon nanomaterials investigated in this work are toxic to the murine J774 cell line. This is consistent with the previous results that CNT and Printex U are toxic to J774 cells (Kumarathasan et al., 2012) and graphene oxide can induce dose-dependent cell death in normal human lung fibroblasts (HLFs), macrophages (THP-1 and J744A), epithelial (BEAS-2B) cells, lung cancer cells (A549), etc. (Zhang et al., 2016; Li et al., 2018). At the same time, the BrdU activities decreased as a function of the dose of carbon nanomaterials, which means they are an inhibitor for cell proliferation of murine J744 cells (Cappella et al., 2015). In addition, except for SB4A, other carbon nanomaterials showed significant increases in LDH. This means that the integrity of

cell membrane decreased when J774 cells were exposed to these engineered carbon nanomaterials, while the cell membrane might be intact when exposed to SB4A (Cho et al., 2008; Kumarathasan et al., 2015). This might be related to lipid peroxidation induced by these engineered particles (Li et al., 2018) and the nonspherical feature of these engineered particles as observed in Fig. S1. These results are also consistent with the previous study that observed CNT cytotoxicity ranking was assay dependent (Kumarathasan et al., 2015).

As shown in Fig. S3, all these carbon nanomaterials revealed negative zeta potential from −42 to −20 mV. SB4A, graphene oxide and SWCNT-COOH almost had the same zeta potential (−42 mV), while SWCNT, SWCNT-OH and graphene showed comparable zeta potentials. This observation suggested the stability of dispersed SB4A, graphene oxide and SWCNT-COOH in water and the interaction between these particles with cells was comparable. However, the cytotoxicity of SB4A, graphene and SWCNT showed an increasing trend regarding the metabolic activity of J774 cells (Fig. 2). This can be explained by the different mode of action (MOA) when the cells were exposed to different types of nanomaterials. For example, adhesions and/or covering on cells could be the main MOA for graphene and graphene oxide (2-D structure) (Gupta et al., 2019; Keshavan et al., 2017), while for carbon nanotubes (1-D structure), piercing and/or internalization by cells could be the main MOA (Lacerda et al., 2013). This means morphology should play a role in determining the cytotoxicity of the carbon nanomaterials studied in this work. Therefore, in the following section we mainly discuss the cytotoxicity among these materials having the same dimension, such as SWCNT-OH and SWCNT-COOH versus SWCNT and graphene oxide versus graphene.

It should be noted that oxidized carbon nanomaterials including graphene oxide, SWCNT-OH and SWCNT-COOH showed weaker reduction of ATP ratio for J774 cells than the counterparts (Fig. 2). These results suggested that functionalized carbon nanomaterials caused a low cytotoxicity of murine J774 cell line regarding cell apoptosis, while a stronger toxicity was demonstrated for cell proliferation and membrane integrity. This finding was true, in particular, for graphene oxide. However, we did not observe a clear dependence of cytotoxicity to the murine J774 cell line on the morphology, the transition metal content, the OC content or the content of oxygen-containing species on the surface of carbon nanomaterials, although oxidized CB materials showed reduced toxicity to the J774 cell lines as far as metabolic activity was considered. In particular, the difference in surface oxygen content between graphene oxide and graphene was much higher than that between SWCNT-OH/SWCNT-COOH and SWCNT (Fig. 5a), while the differences in metabolic activity to the J774 cell line between graphene oxide and graphene were similar to those between SWCNT-OH/SWCNT-COOH and SWCNT. The pathways of cellular toxicity induced by particles reside in both oxidative stress (ROS) and non-oxidative stress dependent (Shvedova et al., 2012). Oxidative stress leads to selective oxidation of mitochondrial cardiolipin (CL), NADPH oxidase (nicotinamide adenine dinucleotide phosphate oxidase) activation and myeloperoxidase (MPO) activation in neutrophils, while non-oxidative stress results from interference with mitotic spindle and actin cytoskeleton, and steric hindrance of ion channels. The interaction between target cells and particles should be more complicated than that between DTT and particles. As discussed above, the cytotoxicity of nanoparticles relied on not only the mode of action but also the chemical nature of particles. Therefore, the different responses of the oxidation potential and the cytotoxicity to the epoxide content in these carbon materials might be accounted for by different mechanisms of toxicity among these assays.

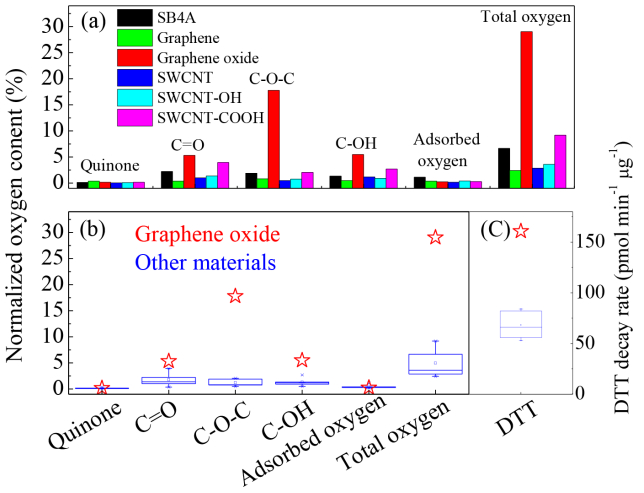

Figure 5. **(a)** Distribution of oxygen-containing species on the tested carbon nanomaterials; **(b)** comparison of oxygen-containing species and **(c)** DTT decay rate between graphene oxide and other carbon nanomaterials.

The DTT decay rate (Fig. 1) did not show obvious dependence on their morphologies in this work. For example, except for graphene oxide, the DTT decay rates were comparable among all the other materials regardless of the morphology. Graphene and graphene oxide showed similar particle sizes, graphene layers and morphologies (Fig. S1), while they showed totally different toxicity as shown in Fig. 1. Transition metals in the particles have been identified to be the important contributor to ROS generation (McWhinney et al., 2013b; Li et al., 2003). It should be noted that although the metal content of SB4A was very low compared to other materials (Fig. S4), the DTT decay rate of SB4A was still comparable with these engineered carbon nanomaterials, except for graphene oxide as shown in Fig. 1. On the other hand, SWCNTs had the highest metal content, while graphene oxide rather than SWCNTs showed the strongest DTT decay rate. In addition, the soluble metal contents were in the following order: SWCNT-COOH > SWCNT > SB4A > graphene ox-

ide > graphene > SWCNT-OH (Fig. S4b), after being sonicated for 30 min in water. Graphene oxide ($103.7\,\mu g\,g^{-1}$) did not show a significant difference compared to SB4A ($106.3\,\mu g\,g^{-1}$) or graphene ($93.7\,\mu g\,g^{-1}$). These results indicated that the high oxidative potential of graphene oxide relative to other materials cannot be attributed to their difference in bounded or soluble transition metals. This can be explained by the following reasons. First, metal content was measured after digested with 1 : 3 HNO_3/HCl. The speciation of metals should be quite different from that presenting in the pristine carbon nanomaterials. For example, the contents of soluble metal ions after sonicated for 30 min (Fig. S4b) varied from 0 to $356\,\mu g\,g^{-1}$. These values were much lower than the corresponding metal contents of digested samples as shown in Fig. S4a. Second, metals might be in the inner pores of carbon nanomaterials. This will decrease the efficiency of metals to generate ROS. Finally, the concentration of carbon nanomaterials was 10–40 $\mu g\,mL^{-1}$ in DTT assay tests. This meant that the concentration of transition metals was at the nanogram per milliliter ($ng\,mL^{-1}$) level even if all of the transition metals were available. The low concentration of metals released might lead to negligible contribution to ROS formation. This was further confirmed by the very low DTT decay rate of the SWCNT filtered solution ($1.66 \pm 0.15\,pmol\,min^{-1}\,\mu g^{-1}$) compared to that of SWCNT suspension ($38.9 \pm 8.9\,pmol\,min^{-1}\,\mu g^{-1}$) even though SWCNT had the highest metal concentration (Fig. S4a). This was consistent with the previous conclusions that redox activity originates from the surface of CB or soot particles but not from water-soluble substances (Liu et al., 2015; McWhinney et al., 2013a).

As shown in the inset graph of Fig. 3a, the content of organics cannot explain the sequence of the DTT loss rate (Fig. 1) of these carbon nanomaterials. For example, the content of organics on graphene and graphene oxide were almost the same, while the DTT decay rate of graphene oxide was about 2.5 times as that of graphene (Fig. 1) This means the different DTT loss rates observed in this study cannot be explained by the adsorbed organics among these materials. Figure 5a summarizes the distribution of the abovementioned oxygen species normalized to O atoms in these carbon nanomaterials. At the present time, the relative sensitivity factors for each oxygen-containing species are unavailable. Similar to the method used in the literature (Chen et al., 2017; Schuster et al., 2011), we simply assumed all these oxygen-containing species in the envelope of O1s having the same relative sensitivity factors. It should be reliable when semi-quantitatively comparing the contents of oxygen-containing species among different samples although additional uncertainties might be introduced for the calculated oxygen content. Highly conjugated form of carbonyl oxygen (quinone) and adsorbed oxygen contributed little to the total oxygen on the surface (< 1 %), while C=O, C−O−C and C−OH were predominating oxygen-containing species. Our results agree well with the previous work that C=O, C−O−C and C−OH dominated oxygen-containing species on natural chars, diesel soot, hexane soot and activated charcoal (Langley et al., 2006). Although quinone has been recognized to contribute to ROS generation on the surface of fine particles (Kumagai et al., 2002; Li et al., 2002b), the content of quinone was lower than 0.35 % and showed little difference among all of these tested carbon nanomaterials (Fig. 5a and b). It did contribute to ROS generation for adsorbed oxygen content. Therefore, we can conclude that the very high DTT decay rates of graphene oxide compared to other carbon nanomaterials as shown in Fig. 5c cannot be explained by the content of quinone or adsorbed oxygen.

As shown in Fig. 5a, the total oxygen contents of SB4A, graphene, SWCNT, SWCNT-OH and SWCNT-COOH were 6.68 %, 2.41 %, 2.88 %, 3.60 % and 9.21 %, respectively. They were comparable with that of diesel soot (2.1 %–12.2 %) (Schuster et al., 2011). However, the oxygen content of graphene oxide (29.0 %) was significantly higher than the other carbon nanomaterials (Fig. 5a). At the same time, the distribution pattern of the surface species on graphene oxide was quite different from the other carbon nanomaterials. Figure 5b compared the content of the oxygen-containing species of graphene oxide with other carbon nanomaterials. The red stars indicate the content of oxygen-containing species in graphene oxide, while the blue boxes show those of other carbon nanomaterials. It can be seen that the content of quinone and adsorbed oxygen show no difference between graphene oxide and other carbon nanomaterials. The concentrations of C=O and C−OH in graphene oxide was slightly higher than those in the other carbon nanomaterials. However, the content of epoxide in graphene oxide was significantly higher than the other carbon nanomaterials. The content of epoxide in graphene oxide normalized to O atoms was 20.8 %, which was 71.7 % of its total oxygen content (Fig. 5b), while it was less than 2.7 % in other carbon nanomaterials. This corresponded well to the high DTT decay rates of graphene oxide ($160.7\,pmol\,min^{-1}\,\mu g^{-1}$) compared to other carbon nanomaterials (less than $60\,pmol\,min^{-1}\,\mu g^{-1}$) as shown in Fig. 5c. It should be noted that the content of epoxide was not linearly correlated to the DTT activity. This can be explained by the typical nonlinear relationship between the dose of toxicant and toxicity (Antinolo et al., 2015). It should be pointed out that multiple parameters of particles may have an influence on its toxicity, in particular on the cytotoxicity. For example, particle size and morphology may have influences on the material mobility and uptake by cells. Although the observed toxicity, including DTT activity and cytotoxicity, could be a coincidence of the chemical composition, functional groups and morphology of these particles, the above results at least imply that these physiochemical properties (such as morphology, metal content and OC content) should not be crucial factors for the toxicity of these carbon nanomaterials because it is difficult to observe an obvious dependence of the toxicity on these factors. In the meantime, we can propose that epox-

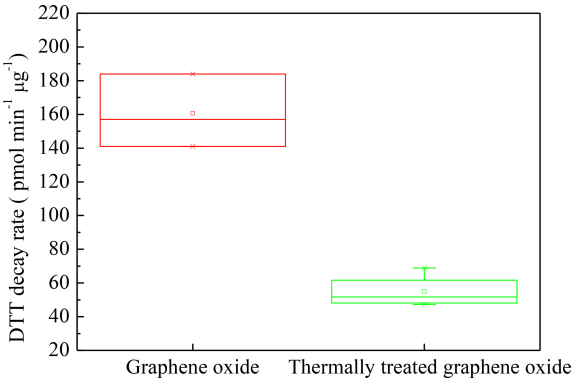

Figure 6. DTT decay rate for graphene oxide and thermally treated graphene oxide in N_2 flow at 200 °C.

ides in graphene oxide are mainly responsible for the high ROS activity of graphene oxide. The high ROS formation potential of graphene oxide might also explain its strong cytotoxicity to the J774 cell line regarding the cell membrane.

To further confirm this assumption, we measured ROS activity of the thermally treated graphene oxide at 200 °C in nitrogen flow because the C−O−C (epoxide) structure can be broken under this condition as shown in Fig. 3, and discussed above. XPS spectra confirmed the break of epoxide by the fact that the content of epoxide in thermally treated graphene oxide decreased to 4.3 % from 20.9 % in graphene oxide as shown in Figs. S5 and S6. In addition, TEM results also show that graphene oxide broke into small sheets, whose morphology and particle size were close to that of SB4A (Fig. S1). At the same time, the DTT decay rate of the thermally treated graphene oxide decreased to 54.9 ± 9.8 pmol min^{-1} μg^{-1} (Fig. 6). This value was comparable to the DTT decay rates of other carbon nanomaterials, in particular graphene (58.5 ± 6.6 pmol min^{-1} μg^{-1}) (Fig. 1), while it was significantly lower than graphene oxide ($160.7.0 \pm 21.7$ pmol min^{-1} μg^{-1}) as shown in Fig. 6. It should be noted that the total oxygen content of thermally treated graphene oxide was 19.3 %, which was lower than that of graphene oxide (29.0 %) but significantly higher than that of other carbon nanomaterials. However, the DTT decay rate of thermally treated graphene oxide was still comparable with other carbon nanomaterials. This further highlights the importance of functional groups in the DTT decay rate. Therefore, this means that epoxides in graphene oxide are the highly reactive sites for ROS formation on the surface. It is for the first time observed that epoxide is a highly reactive site for ROS formation besides quinone on carbon nanomaterials. This result is also consistent with the previous finding that epoxides in graphene oxide can oxidize SO_2 to sulfate (He and He, 2016), although their oxidation mechanism might be different.

If other ethers are present in the carbon nanomaterials, it should be noted that they should also contribute to the O1s band, which might be close to that of epoxide. However, at the present time, it is recognized that oxygen-containing species including epoxide, hydroxyl, carbonyl and carboxylic groups are present in graphene layers (Inagaki and Kang, 2014; Hunt et al., 2012). Epoxide should dominate the band at 532.6 eV compared to ethers (Hunt et al., 2012). In particular, the TGA results also support the high content of epoxide in graphene oxide. For other samples in this work, other ethers might overestimate their contents of epoxide. However, this should not have an influence on our conclusion that epoxides are related to the high oxidation potential of graphene oxide.

Recently, environmentally persistent free radicals (EPFRs, surface-stabilized metal–radical complexes characterized by an oxygen-centered radical; Dugas et al., 2016) have been identified in different sources of particles including biomass or coal combustion, diesel and gasoline exhaust, ambient $PM_{2.5}$, and polymers (Balakrishna et al., 2009; Truong et al., 2010; Dugas et al., 2016). However, it is unclear whether epoxide in graphene oxide observed in this study contributes to the EPFR formation. This needs to be investigated in the future.

5 Conclusion and atmospheric implications

Oxidation is a useful method to obtain functionalized CB materials with distinctive performance in industry. This process unusually leads to formation of carbonyls, hydroxyls, carboxylic acids, esters, ethers and epoxides on the surface of CB or soot particles. Previous work has found that oxidation of carbon nanomaterials (SWCNT) by O_3 or OH under atmosphere-related conditions has little influence on their oxidative potential or cytotoxicity although carbonyls, carboxylic acids and esters were formed (Liu et al., 2015). Similarly, surface functionalization was observed for commercial CB materials by ozone oxidation, while an increase in the cytotoxicity of murine macrophages and release of inflammation markers upon exposure to the oxidized CB were not observed (Peebles et al., 2011). However, some other studies observed that the oxidation process enhanced the oxidation potential (Li et al., 2015, 2013; Antinolo et al., 2015) as well as the cytotoxicity (Holder et al., 2012) of CB and soot particles. Using model carbon nanomaterials with different dominant surface functionalities, we have found that hydroxyl and carboxyl functionalized CB particles had little influence on their oxidation potential, while epoxide functionalized CB (graphene oxide) led to a very strong oxidation potential. Epoxide has been identified as a surface product on SWCNT when treated with high concentration of ozone (Mawhinney et al., 2000; Yim and Johnson, 2009). Besides carboxylic acids, esters (Liu et al., 2015), ketones, lactone and anhydride species (Liu et al., 2010; Han et al., 2012b), epoxides have also been identified as the surface product during oxidation of SWCNTs in atmosphere-relevant condi-

tions (Liu et al., 2015). On the other hand, graphene oxide is an important commercial product, which showed a strong oxidation potential as observed in this work. This means that exposure to epoxide-containing carbon materials should lead to high health risks in regards to oxidation potential. Therefore, Mussel-inspired chemistry is necessary for fabrication of functional materials and decreasing their toxicity and for biomedical applications (Y. Liu et al., 2014; Zhang et al., 2012).

It has been found that CB particles (Printex 90) can induce opening of plasma membrane calcium channels leading to a calcium influx and cause significant release of proinflammatory cytokine TNF-α (tumor necrosis factor) by the murine J774 cells (Brown et al., 2004), subsequently potentially induce migration of macrophages (Barlow et al., 2005). This could initiate the recruitment of inflammatory cells to sites of particle deposition and the subsequent removal of the particles by macrophages. The metabolic activity of these hydroxy-, carboxylic-acid- and epoxide-functionalized carbon nanomaterials increased when compared with the corresponding sample as observed in this work. This implies that functionalization of carbon nanomaterials might not pose an enhanced cytotoxicity risk to macrophages when compared with the corresponding control materials although the oxidized carbon nanomaterials were still toxic as far as metabolic activity was considered. However, the oxidized carbon nanomaterials might pose enhanced cytotoxicity to macrophages regarding membrane integrity and DNA synthesis. It should be pointed out that exposure experiments were performed under high particle concentration with short exposure time in this work. More work needs to be done at low particle concentration with long exposure time in the future. On the other hand, the interaction between particles and biological entities such as proteins or cells has not been considered in this work. Therefore, the in vivo toxicological effect of these functionalized particles needs to be further evaluated in the future. Finally, condensation of co-emitted species and photooxidation products is particularly rapid under conditions of soot emissions (Johnson et al., 2005; Adachi et al., 2010; Peng et al., 2016). In our previous work, it was found that condensation processes significantly decreased the oxidation potential of SWCNTs (Liu et al., 2015). A recent work has also found that condensation of organic aerosol leads to a decrease in oxidation potential of engineered nanoparticles (Liu et al., 2019). Therefore, the contribution of functional groups to the oxidation potential should be greatly influenced by condensation of co-emitted species and photooxidation products in the atmosphere. This might be dependent on the carbon nanomaterial itself and needs to be investigated in the future.

Data availability. The experimental data are available upon request to the corresponding authors.

Supplement. The supplement related to this article is available online at: https://doi.org/10.5194/acp-19-8175-2019-supplement.

Author contributions. YL, HH and SL designed the experiments. YL wrote the paper. YL, HJ and YG did the DTT assay tests. CL and LW did the cytotoxicity assessments. HJ and BZ performed the characterization of samples.

Competing interests. The authors declare that they have no conflict of interest.

Acknowledgements. This research was financially supported by the National Natural Science Foundation of China (41877306 and 91543109) and the Fundamental Research Funds for the Central Universities (PT1907). YL thanks the Beijing University of Chemical Technology for financial support.

Financial support. This research was financially supported by the National Natural Science Foundation of China (41877306 and 91543109) and the Fundamental Research Funds for the Central Universities (PT1907).

Review statement. This paper was edited by Markus Ammann and reviewed by two anonymous referees.

References

Adachi, K., Chung, S. H., and Buseck, P. R.: Shapes of soot aerosol particles and implications for their effects on climate, J. Geophys. Res.-Atmos., 115, D15206, https://doi.org/10.1029/2009jd012868, 2010.

Andreae, M. O. and Gelencser, A.: Black carbon or brown carbon? The nature of light-absorbing carbonaceous aerosols, Atmos. Chem. Phys., 6, 3131–3148, https://doi.org/10.5194/acp-6-3131-2006, 2006.

Antinolo, M., Willis, M. D., Zhou, S., and Abbatt, J. P. D.: Connecting the oxidation of soot to its redox cycling abilities, Nat. Commun., 6, 6812, https://doi.org/10.1038/ncomms7812, 2015.

Apicella, B., Barbella, R., Ciajolo, A., and Tregrossi, A.: Comparative analysis of the structure of carbon materials relevant in combustion, Chemosphere, 51, 1063–1069, https://doi.org/10.1016/S0045-6535(02)00715-4, 2003.

Balakrishna, S., Lomnicki, S., McAvey, K. M., Cole, R. B., Dellinger, B., and Cormier, S. A.: Environmentally persistent free radicals amplify ultrafine particle mediated cellular oxidative stress and cytotoxicity, Part. Fibre Toxicol., 6, 11, https://doi.org/10.1186/1743-8977-6-11, 2009.

Barlow, P. G., Clouter-Baker, A., Donaldson, K., MacCallum, J., and Stone, V.: Carbon black nanoparticles induce type II epithelial cells to release chemotaxins for alveolar macrophages, Part. Fibre Toxicol., 2, 11, https://doi.org/10.1186/1743-8977-2-11, 2005.

Baumgartner, J., Zhang, Y., Schauer, J. J., Huang, W., Wang, Y., and Ezzati, M.: Highway proximity and black carbon from cookstoves as a risk factor for higher blood pressure in rural China, P. Natl. Acad. Sci. USA, 111, 13229–13234, https://doi.org/10.1073/pnas.1317176111, 2014.

Brown, D. M., Donaldson, K., and Stone, V.: Effects of PM_{10} in human peripheral blood monocytes and J774 macrophages, Respir. Res., 5, 29, https://doi.org/10.1186/1465-9921-5-29, 2004.

Cain, J. P., Gassman, P. L., Wang, H., and Laskin, A.: Micro-FTIR study of soot chemical composition-evidence of aliphatic hydrocarbons on nascent soot surfaces, Phys. Chem. Chem. Phys., 12, 5206–5218, https://doi.org/10.1039/b924344e, 2010.

Cappella, P., Gasparri, F., Pulici, M., and Moll, J.: Cell proliferation method: click chemistry based on brdu coupling for multiplex antibody staining, Curr. Protoc. Cy., 72, 7.34.31–17, https://doi.org/10.1002/0471142956.cy0734s72, 2015.

Cedervall, T., Lynch, I., Lindman, S., Berggård, T., Thulin, E., Nilsson, H., Dawson, K. A., and Linse, S.: Understanding the nanoparticle–protein corona using methods to quantify exchange rates and affinities of proteins for nanoparticles, P. Natl. Acad. Sci. USA, 104, 2050–2055, https://doi.org/10.1073/pnas.0608582104, 2007.

Charrier, J. G. and Anastasio, C.: On dithiothreitol (DTT) as a measure of oxidative potential for ambient particles: evidence for the importance of soluble transition metals, Atmos. Chem. Phys., 12, 9321–9333, https://doi.org/10.5194/acp-12-9321-2012, 2012.

Chen, D., He, D., Lu, J., Zhong, L., Liu, F., Liu, J., Yu, J., Wan, G., He, S., and Luo, Y.: Investigation of the role of surface lattice oxygen and bulk lattice oxygen migration of cerium-based oxygen carriers: XPS and designed H_2-TPR characterization, Appl. Catal. B: Environ., 218, 249–259, https://doi.org/10.1016/j.apcatb.2017.06.053, 2017.

Cho, A. K., Sioutas, C., Miguel, A. H., Kumagai, Y., Schmitz, D. A., Singh, M., Eiguren-Fernandez, A., and Froines, J. R.: Redox activity of airborne particulate matter at different sites in the Los Angeles Basin, Environ. Res., 99, 40–47, https://doi.org/10.1016/j.envres.2005.01.003, 2005.

Cho, M.-H., Niles, A., Ruili, H., Inglese, J., Austin, C. P., Riss, T., and Xia, M.: A bioluminescent cytotoxicity assay for assessment of membrane integrity using a proteolytic biomarker, Toxicol. In Vitro., 22, 1099–1106, 2008.

Corbin, J. C., Lohmann, U., Sierau, B., Keller, A., Burtscher, H., and Mensah, A. A.: Black carbon surface oxidation and organic composition of beech-wood soot aerosols, Atmos. Chem. Phys., 15, 11885–11907, https://doi.org/10.5194/acp-15-11885-2015, 2015.

Dugas, T. R., Lomnicki, S., Cormier, S. A., Dellinger, B., and Reams, M.: Addressing emerging risks: scientific and regulatory challenges associated with environmentally persistent free radicals, Int. J. Environ. Res. Public Health, 13, 537, https://doi.org/10.3390/ijerph13060573, 2016.

Fang, T., Verma, V., Bates, J. T., Abrams, J., Klein, M., Strickland, M. J., Sarnat, S. E., Chang, H. H., Mulholland, J. A., Tolbert, P. E., Russell, A. G., and Weber, R. J.: Oxidative potential of ambient water-soluble PM2.5 in the southeastern United States: contrasts in sources and health associations between ascorbic acid (AA) and dithiothreitol (DTT) assays, Atmos. Chem. Phys., 16, 3865–3879, https://doi.org/10.5194/acp-16-3865-2016, 2016.

Foroozandeh, P. and Aziz, A. A.: Insight into cellular uptake and intracellular trafficking of nanoparticles, Nanoscale Res. Lett., 13, 339–339, https://doi.org/10.1186/s11671-018-2728-6, 2018.

Golberg, D., Costa, P., Wang, M. S., Wei, X. L., Tang, D. M., Xu, Z., Huang, Y., Gautam, U. K., Liu, B. D., Zeng, H. B., Kawamoto, N., Zhi, C. Y., Mitome, M., and Bando, Y.: Nanomaterial engineering and property studies in a transmission electron microscope, Adv. Mater., 24, 177–194, https://doi.org/10.1002/adma.201102579, 2012.

Gupta, P., Agrawal, A., Murali, K., Varshney, R., Beniwal, S., Manhas, S., Roy, P., and Lahiri, D.: Differential neural cell adhesion and neurite outgrowth on carbon nanotube and graphene reinforced polymeric scaffolds, Mater. Sci. Eng. C-Mater. Biol. Appl., 97, 539–551, https://doi.org/10.1016/j.msec.2018.12.065, 2019.

Hadrup, N., Bengtson, S., Jacobsen, N. R., Jackson, P., Nocun, M., Saber, A. T., Jensen, K. A., Wallin, H., and Vogel, U.: Influence of dispersion medium on nanomaterial-induced pulmonary inflammation and DNA strand breaks: investigation of carbon black, carbon nanotubes and three titanium dioxide nanoparticles, Mutagenesis, 32, 581–597, https://doi.org/10.1093/mutage/gex042, 2017.

Han, C., Liu, Y., Liu, C., Ma, J., and He, H.: Influence of combustion conditions on hydrophilic properties and microstructure of flame soot, J. Phys. Chem. A, 116, 4129–4136, https://doi.org/10.1021/jp301041w, 2012a.

Han, C., Liu, Y., Ma, J., and He, H.: Effect of soot microstructure on its ozonization reactivity, J. Chem. Phys., 2012, 084507, https://doi.org/10.1063/1.4747190, 2012b.

He, G. and He, H.: DFT studies on the heterogeneous oxidation of SO_2 by oxygen functional groups on graphene, Phys. Chem. Chem. Phys., 18, 31691–31697, 2016.

Helland, A., Wick, P., Koehler, A., Schmid, K., and Som, C.: Reviewing the environmental and human health knowledge base of carbon nanotubes, Environ. Health Perspect., 115, 1125–1131, 2007.

Holder, A. L., Carter, B. J., Goth–Goldstein, R., Lucas, D., and Koshland, C. P.: Increased cytotoxicity of oxidized flame soot, Atmos. Pollu. Res. , 3, 25–31, 2012.

Hu, L., Hecht, D. S., and Grüner, G.: Carbon nanotube thin films: Fabrication, properties, and applications, Chem. Rev., 110, 5790–5844, https://doi.org/10.1021/cr9002962, 2010.

Hunt, A., Dikin, D. A., Kurmaev, E. Z., Boyko, T. D., Bazylewski, P., Chang, G. S., and Moewes, A.: Epoxide speciation and functional group distribution in graphene oxide paper-like materials, Adv. Funct. Mater., 22, 3950–3957, https://doi.org/10.1002/adfm.201200529, 2012.

Inagaki, M. and Kang, F.: Materials science and engineering of carbon: Fundamentals (2nd Ed), Butterworth-Heinemann, Oxford, 542 pp., 2014.

Johnson, K. S., Zuberi, B., Molina, L. T., Molina, M. J., Iedema, M. J., Cowin, J. P., Gaspar, D. J., Wang, C., and Laskin, A.: Processing of soot in an urban environment: case study from the Mexico City Metropolitan Area, Atmos. Chem. Phys., 5, 3033–3043, https://doi.org/10.5194/acp-5-3033-2005, 2005.

Keshavan, S., Oropesa-Nunez, R., Diaspro, A., Canale, C., and Dante, S.: Adhesion and migration of CHO cells on micropatterned single layer graphene, 2D Mater., 4, 025022, https://doi.org/10.1088/2053-1583/aa57e9, 2017.

Kim, H., Park, K., and Lee, M.-Y.: Biocompatible dispersion methods for carbon black, Toxicol. Res., 28, 209–216, 2012.

Koike, E. and Kobayashi, T.: Chemical and biological oxidative effects of carbon black nanoparticles, Chemosphere, 65, 946–951, https://doi.org/10.1016/j.chemosphere.2006.03.078, 2006.

Koromilas, N. D., Lainioti, G. C., Gialeli, C., Barbouri, D., Kouravelou, K. B., Karamanos, N. K., Voyiatzis, G. A., and Kallitsis, J. K.: Preparation and toxicological assessment of functionalized carbon nanotube-polymer hybrids, Plos One, 9, e107029, https://doi.org/10.1371/journal.pone.0107029, 2014.

Kumagai, Y., Koide, S., Taguchi, K., Endo, A., Nakai, Y., Yoshikawa, T., and Shimojo, N. C.: Oxidation of proximal protein sulfhydryls by phenanthraquinone, a component of diesel exhaust particles, Chem. Res. Toxicol., 15, 483–489, 2002.

Kumarathasan, P., Das, D., Salam, M. A., Mohottalage, S., DeSilva, N., Simard, B., and Vincent, R.: Mass spectrometry-based proteomic assessment of the in vitro toxicity of carbon nanotubes, Curr. Topics Biochem. Res., 14, 15–27, 2012.

Kumarathasan, P., Breznan, D., Das, D., Salam, M. A., Siddiqui, Y., MacKinnon-Roy, C., Guan, J., de Silva, N., Simard, B., and Vincent, R.: Cytotoxicity of carbon nanotube variants: A comparative in vitro exposure study with A549 epithelial and J774 macrophage cells, Nanotoxicology, 9, 148–161, https://doi.org/10.3109/17435390.2014.902519, 2014.

Kumarathasan, P., Breznan, D., Das, D., Salam, M. A., Siddiqui, Y., MacKinnon-Roy, C., Guan, J., de Silva, N., Simard, B., and Vincent, R.: Cytotoxicity of carbon nanotube variants: A comparative in vitro exposure study with A549 epithelial and J774 macrophage cells, Nanotoxicology, 9, 148–161, https://doi.org/10.3109/17435390.2014.902519, 2015.

Kuznetsova, A., Popova, I., Yates, J. T., Bronikowski, M. J., Huffman, C. B., Liu, J., Smalley, R. E., Hwu, H. H., and Chen, J. G.: Oxygen-containing functional groups on single-wall carbon nanotubes:? nexafs and vibrational spectroscopic studies, J. Am. Chem. Soc., 123, 10699–10704, https://doi.org/10.1021/ja011021b, 2001.

Lacerda, L., Ali-Boucetta, H., Kraszewski, S., Tarek, M., Prato, M., Ramseyer, C., Kostarelos, K., and Bianco, A.: How do functionalized carbon nanotubes land on, bind to and pierce through model and plasma membranes, Nanoscale, 5, 10242–10250, https://doi.org/10.1039/c3nr03184e, 2013.

Lam, J., Herant, M., Dembo, M., and Heinrich, V.: Baseline Mechanical characterization of J774 macrophages, Biophys. J., 96, 248–254, 2009.

Langley, L. A., Villanueva, D. E., and Fairbrother, D. H.: Quantification of surface oxides on carbonaceous materials, Chem. Mater., 18, 169–178, 2006.

Lara-Martinez, L. A., Masso, F., Gonzalez, E. P., Garcia-Pelaez, I., Contreras-Ramos, A., Valverde, M., Rojas, E., Cervantes-Sodi, F., and Hernandez-Gutierrez, S.: Evaluating the biological risk of functionalized multiwalled carbon nanotubes and functionalized oxygen-doped multiwalled carbon nanotubes as possible toxic, carcinogenic, and embryotoxic agents, Inter. J. Nanomed., 12, 7695–7707, https://doi.org/10.2147/ijn.s144777, 2017.

Lee, Y. S., Park, S. H., Lee, J. C., and Ha, K.: Influence of microstructure in nitrile polymer on curing characteristics and mechanical properties of carbon black-filled rubber composite for seal applications, J. Elastomer Plast., 48, 659–676, https://doi.org/10.1177/0095244315613621, 2016.

Li, N., Kim, S., Wang, M., Froines, J., Sioutas, C., and Nel, A.: Use of a stratified oxidative stress model to study the biological effects of ambient concentrated and diesel exhaust particulate matter, Inhal. Toxicol., 14, 459–486, https://doi.org/10.1080/08958370175367857l, 2002a.

Li, N., Wang, M., Oberley, T. D., Sempf, J. M., and Nel, A. E.: Comparison of the pro-oxidative and proinflammatory effects of organic diesel exhaust particle chemicals in bronchial epithelial cells and macrophages, J. Immunol., 169, 4531–4541, 2002b.

Li, N., Sioutas, C., Cho, A., Schmitz, D., Misra, C., Sempf, J., Wang, M., Oberley, T., Froines, J., and Nel, A.: Ultrafine particulate pollutants induce oxidative stress and mitochondrial damage, Environ. Health Perspect., 111, 455–460, 2003.

Li, Q., Wyatt, A., and Kamens, R. M.: Oxidant generation and toxicity enhancement of aged-diesel exhaust, Atmos. Environ., 43, 1037–1042, https://doi.org/10.1016/j.atmosenv.2008.11.018, 2009.

Li, Q., Shang, J., and Zhu, T.: Physicochemical characteristics and toxic effects of ozone-oxidized black carbon particles, Atmos. Environ., 81, 68–75, https://doi.org/10.1016/j.atmosenv.2013.08.043, 2013.

Li, Q., Shang, J., Liu, J., Xu, W., Feng, X., Li, R., and Zhu, T.: Physicochemical characteristics, oxidative capacities and cytotoxicities of sulfate-coated, 1,4-NQ-coated and ozone-aged black carbon particles, Atmos. Res., 153, 535–542, https://doi.org/10.1016/j.atmosres.2014.10.005, 2015.

Li, R. B., Guiney, L. M., Chang, C. H., Mansukhani, N. D., Ji, Z. X., Wang, X., Liao, Y. P., Jiang, W., Sun, B. B., Hersam, M. C., Nel, A. E., and Xia, T.: Surface oxidation of graphene oxide determines membrane damage, lipid peroxidation, and cytotoxicity in macrophages in a pulmonary toxicity model, ACS Nano, 12, 1390–1402, https://doi.org/10.1021/acsnano.7b07737, 2018.

Liu, Q., Baumgartner, J., Zhang, Y., Liu, Y., Sun, Y., and Zhang, M.: Oxidative potential and inflammatory impacts of source apportioned ambient air pollution in beijing, Environ. Sci. Technol., 48, 12920–12929, https://doi.org/10.1021/es5029876, 2014.

Liu, Q., Liggio, J., Breznan, D., Thomson, E. M., Kumarathasan, P., Vincent, R., Li, K., and Li, S.-M.: Oxidative and toxicological evolution of engineered nanoparticles with atmospherically relevant coatings, Environ. Sci. Technol., 53, 3058–3066, https://doi.org/10.1021/acs.est.8b06879, 2019.

Liu, Y., Liu, C., Ma, J., Ma, Q., and He, H.: Structural and hygroscopic changes of soot during heterogeneous reaction with O_3, Phys. Chem. Chem. Phys., 12, 10896–10903, 2010.

Liu, Y., Ai, K. and Lu, L.: Polydopamine and its derivative materials: synthesis and promising applications in energy, environmental, and biomedical fields, Chem. Rev., 114, 5057–5115, https://doi.org/10.1021/cr400407a, 2014.

Liu, Y., Liggio, J., Li, S.-M., Breznan, D., Vincent, R., Thomson, E. M., Kumarathasan, P., Das, D., Abbatt, J., Antiñolo, M., and Russell, L.: Chemical and toxicological evolution of carbon nanotubes during atmospherically relevant aging processes, Environ. Sci. Technol., 49, 2806–2814, https://doi.org/10.1021/es505298d, 2015.

Long, C. M., Nascarella, M. A., and Valberg, P. A.: Carbon black vs. black carbon and other airborne materials containing elemental carbon: Physical and chemical distinctions, Environ. Pollut., 181, 271–286, https://doi.org/10.1016/j.envpol.2013.06.009, 2013.

Maruyama, T.: Current status of single-walled carbon nanotube synthesis from metal catalysts by chemical vapor deposition, Mater. Express, 8, 1–20, https://doi.org/10.1166/mex.2018.1407, 2018.

Mawhinney, D. B., Naumenko, V., Kuznetsova, A., Yates, J. T., Liu, J., and Smalley, R. E.: Infrared spectral evidence for the etching of carbon nanotubes: Ozone oxidation at 298 K, J. Am. Chem. Soc., 122, 2383–2384, https://doi.org/10.1021/ja994094s, 2000.

McWhinney, R. D., Badali, K., Liggio, J., Li, S.-M., and Abbatt, J. P. D.: Filterable redox cycling activity: a comparison between diesel exhaust particles and secondary organic aerosol constituents, Environ. Sci. Technol., 47, 3362–3369, https://doi.org/10.1021/es304676x, 2013a.

McWhinney, R. D., Zhou, S., and Abbatt, J. P. D.: Naphthalene SOA: redox activity and naphthoquinone gas–particle partitioning, Atmos. Chem. Phys., 13, 9731–9744, https://doi.org/10.5194/acp-13-9731-2013, 2013b.

Muckenhuber, H. and Grothe, H.: The heterogeneous reaction between soot and NO_2 at elevated temperature, Carbon, 44, 546–559, 2006.

Nel, A., Xia, T., Määdler, L., and Li, N.: Toxic potential of materials at the nanolevel., Science, 311, 622–627, 2006.

Nienow, A. M. and Roberts, J. T.: Heterogeneos chemsitry of carbon aerosols, Annu. Rev. Phys. Chem., 57, 105–128, 2006.

Niranjan, R. and Thakur, A. K.: The toxicological mechanisms of environmental soot (black carbon) and carbon black: Focus on oxidative stress and inflammatory pathways, Front. Immunol., 8, 763, https://doi.org/10.3389/fimmu.2017.00763, 2017.

Parant, H., Muller, G., Le Mercier, T., Tarascon, J. M., Poulin, P., and Colin, A.: Flowing suspensions of carbon black with high electronic conductivity for flow applications: Comparison between carbons black and exhibition of specific aggregation of carbon particles, Carbon, 119, 10–20, https://doi.org/10.1016/j.carbon.2017.04.014, 2017.

Peebles, B. C., Dutta, P. K., Waldman, W. J., Villamena, F. A., Nash, K., Severance, M., and Nagy, A.: Physicochemical and toxicological properties of commercial carbon blacks modified by reaction with ozone, Environ. Sci. Technol., 45, 10668–10675, 2011.

Peng, J., Hu, M., Guo, S., Du, Z., Zheng, J., Shang, D., Levy Zamora, M., Zeng, L., Shao, M., Wu, Y.-S., Zheng, J., Wang, Y., Glen, C. R., Collins, D. R., Molina, M. J., and Zhang, R.: Markedly enhanced absorption and direct radiative forcing of black carbon under polluted urban environments, P. Natl. Acad. Sci. USA, 113, 4266–4271, https://doi.org/10.1073/pnas.1602310113, 2016.

Popovicheva, O. B., Kireeva, E. D., Shonija, N. K., Vojtisek-Lom, M., and Schwarz, J.: FTIR analysis of surface functionalities on particulate matter produced by off-road diesel engines operating on diesel and biofuel, Environ. Sci. Pollut. Res., 22, 4534–4544, https://doi.org/10.1007/s11356-014-3688-8, 2015.

Sanders, I. J. and Peeten, T. L.: Carbon black: Production, Properties and uses, Chemical engineering methods and technology Materials Science and Technologies Series, Nova Science Publishers, UK, 2011.

Schuster, M. E., Hävecker, M., Arrigo, R., Blume, R., Knauer, M., Ivleva, N. P., Su, D. S., Niessner, R., and Schlögl, R.: Surface sensitive study to determine the reactivity of soot with the focus on the european emission standards IV and VI, J. Phys. Chem. A., 115, 2568–2580, https://doi.org/10.1021/jp1088417, 2011.

Shvedova, A. A., Pietroiusti, A., Fadeel, B., and Kagan, V. E.: Mechanisms of carbon nanotube-induced toxicity: Focus on oxidative stress, Toxicol. Appl. Pharmacol., 261, 121–133, 2012.

Simmons, J. M., Nichols, B. M., Baker, S. E., Marcus, M. S., Castellini, O. M., Lee, C. S., Hamers, R. J., and Eriksson, M. A.: Effect of ozone oxidation on single-walled carbon nanotubes, J. Phys. Chem. B, 110, 7113–7118, https://doi.org/10.1021/jp0548422, 2006.

Somiya, S.: Handbook of advanced ceramics: Materials, application, processing, and properties, 2nd Ed., Academic Press, 2013.

Tiwari, A. J. and Marr, L. C.: The role of atmospheric transformations in determing envrionmental impacts of carbonaceous nanoparticles, J. Environ. Qual., 39, 1883–1895, 2010.

Truong, H., Lomnicki, S., and Dellinger, B.: Potential for misidentification of environmentally persistent free radicals as molecular pollutants in particulate matter, Environ. Sci. Technol., 44, 1933–1939, https://doi.org/10.1021/es902648t, 2010.

Wal, R. L. V., Bryg, V. M., and Hays, M. D.: XPS Analysis of combustion aerosols for chemical composition, surface chemistry, and carbon chemical state, Anal. Chem., 83, 1924–1930, https://doi.org/10.1021/ac102365s, 2011.

Wang, B., Li, K., Jin, W., Lu, Y., Zhang, Y., Shen, G., Wang, R., Shen, H., Li, W., Huang, Y., Zhang, Y., Wang, X., Li, X., Liu, W., Cao, H., and Tao, S.: Properties and inflammatory effects of various size fractions of ambient particulate matter from beijing on A549 and J774A.1 Cells, Environ. Sci. Technol., 47, 10583–10590, https://doi.org/10.1021/es401394g, 2013.

WHO: World Health Organization. Health effects of particulate matter: Policy implications for countries in eastern Europe, Caucasus and central Asia, 2013.

Xia, T., Kovochich, M., Brant, J., Hotze, M., Sempf, J., Oberley, T., Sioutas, C., Yeh, J. I., Wiesner, M. R., and Nel, A. E.: Comparison of the abilities of ambient and manufactured nanoparticles to induce cellular toxicity according to an oxidative stress paradigm, Nano Lett., 6, 1794–1807, https://doi.org/10.1021/nl061025k, 2006.

Yim, W. L. and Johnson, J. K.: Ozone oxidation of single walled carbon nanotubes from density functional theory, J. Phys. Chem. C, 113, 17636–17642, https://doi.org/10.1021/jp908089c, 2009.

Zhang, B., Wei, P., Zhou, Z., and Wei, T.: Interactions of graphene with mammalian cells: Molecular mechanisms and biomedical insights, Adv. Drug Deliv. Rev., 105, 145–162, https://doi.org/10.1016/j.addr.2016.08.009, 2016.

Zhang, X., Wang, S., Xu, L., Feng, L., Ji, Y., Tao, L., Li, S., and Wei, Y.: Biocompatible polydopamine fluorescent organic nanoparticles: facile preparation and cell imaging, Nanoscale, 4, 5581–5584, https://doi.org/10.1039/c2nr31281f, 2012.